

含氮氧自由基的 Gd, Tb, Dy 配合物的合成、结构及磁性

胡 鹏* 吴燕妮 黄期晓 连思绵 付兴慧 何高鹏 陈侠敏

(肇庆学院化学化工学院, 肇庆 526061)

摘要: 合成了一个新颖的氮氧自由基配体, 并用该配体合成了 3 例未见文献报道的氮氧自由基-稀土三自旋单核配合物 $\text{Ln}(\text{hfac})_3(\text{NIT-Ph-4-OCHCH}_3\text{CH}_3)_2$ ($\text{Ln}=\text{Gd}(\mathbf{1}), \text{Tb}(\mathbf{2}), \text{Dy}(\mathbf{3})$; hfac =六氟乙酰丙酮; $\text{NIT-Ph-4-OCHCH}_3\text{CH}_3=4,4,5,5$ -四甲基-2-(4'-异丙氧基苯基)-咪唑啉-3-氧化-1-氧基自由基)。单晶结构分析表明配合物 **1**、**2**、**3** 拥有相似的自由基-稀土-自由基单核结构。对配合物的磁性测试结果表明自由基与稀土之间存在着铁磁相互作用。自由基与自由基之间存在着反铁磁相互作用。

关键词: 氮氧自由基; 稀土; 晶体结构; 磁性

中图分类号: O614.33*9; O614.341; O614.342

文献标识码: A

文章编号: 1001-4861(2016)02-0297-08

DOI: 10.11862/CJIC.2016.032

Gd(III), Tb(III) and Dy(III) Complexes Based on a Nitronyl Nitroxide Radical: Syntheses, Structures and Magnetic Properties

HU Peng* WU Yan-Ni HUANG Qi-Xiao LIAN Si-Mian FU Xing-Hui HE Gao-Peng CHEN Xia-Min

(College of Chemistry and Chemical Engineering, Zhaoqing University, Zhaoqing, Guangdong 526061, China)

Abstract: One novel nitronyl nitroxide radical and its three mononuclear tri-spin compounds $\text{Ln}(\text{hfac})_3(\text{NIT-Ph-4-OCHCH}_3\text{CH}_3)_2$ ($\text{Ln}=\text{Gd}(\mathbf{1}), \text{Tb}(\mathbf{2}), \text{Dy}(\mathbf{3})$; hfac =hexafluoroacetylacetonate; $\text{NIT-Ph-4-OCHCH}_3\text{CH}_3=2-(4\text{-isopropoxyphenyl})-4,4,5,5\text{-tetramethyl-imidazoline-1-oxyl-3-oxide}$) have been successfully prepared and characterized. Single crystal X-ray crystallographic analyses reveal that complexes **1**, **2**, and **3** shows similar radical- Ln(III) -radical structures, which are composed of one $\text{Ln}(\text{hfac})_3$ units and two $\text{NIT-Ph-4-OCHCH}_3\text{CH}_3$ radicals. Magnetic studies reveal that ferromagnetic interactions (between intramolecular Ln and radical) and antiferromagnetic interactions (between the intramolecular radicals) are coexist in these complexes. CCDC: 985443, **1**; 1043098, **2**; 985444, **3**.

Keywords: nitronyl nitroxide radical; lanthanides; crystal structure; magnetic properties

0 Introduction

Single-molecule magnets (SMMs) have attracted many scientists attention in the past two decades^[1-4]. This type of materials are characterized as slow magnetization relaxation caused by the association of large ground state spin (S_T) value with a significant uniaxial (Ising-like) magnetic anisotropy (D), which leads to a significant energy barrier to magnetization reversal (U)^[5-7]. The

SMMs have been found potential applications for the uses of high-density magnetic memories, magnetic refrigeration, quantum computing devices and spintronics at the molecular level^[8-11]. Recently $4f$ metal ions were considered to be good candidates for the construction of SMMs due to their significant magnetic anisotropy arising from the large, unquenched orbital angular momentum. Up to now, a variety of $4f$ metal ions based SMMs have been reported^[12-17].

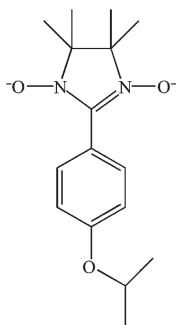
收稿日期: 2015-06-20。收修改稿日期: 2015-12-01。

广东省高校创新强校项目(No.504-20000158)、广东省教育厅科技创新项目(No.2013KJ CX0193)和广东省大创项目(No. 603-60300346)资助。

*通信联系人。E-mail: hp8286799@zqu.edu.cn

Apart from the choice of the metal ions, the ligand design also plays an important role. The use of organic radical ligands in the creation of new magnetic molecular compounds have attracted much attention since the discovery of the first radical-4f SMM by Gatteschi group^[18]. As is well known, the stable radical ligands can generate typically stronger intramolecular magnetic exchange coupling. The strong exchange coupling between lanthanides and radicals generally leads to superior SMMs. Recently, a binuclear Tb(III) complex bridged by a N_2^{3-} radical has been reported with a record blocking temperature of 13.9 K^[19-20]. So far various organic radicals such as nitronyl nitroxide, verdazyl and semiquinone radicals have been reported^[21-25]. However, researches are focused in particular on the nitronyl nitroxide (NIT) family of radicals, because these type of radicals are relatively stable and easy to obtain derivatives with substituents containing donor atoms. Nitronyl nitroxide radicals can act as bidentate ligands through their identical N-O coordination groups and give rise to complexes with different structures. Unfortunately, NIT radicals are poorly donating ligands, thus utilization of strong electron-withdrawing coligands such as hexafluoroacetylacetone (hfac) and trifluoroacetylacetone (tfac) are necessary. However, the steric demand of these coligands restrict the dimensionality of the resulting metal-radical compounds. So, it is easier to get zero- and one-dimensional compounds by this strategy.

To further study the magnetic properties of NIT radical-lanthanide compounds, in this paper we report a novel nitronyl nitroxide radical (Scheme 1) and its corresponding Ln-nitronyl nitroxide compounds Ln(hfac)₃(NIT-Ph-4-OCHCH₃CH₃)₂ (Ln=Gd (**1**), Tb (**2**), Dy



Scheme 1 Molecule structure of NIT-Ph-4-OCHCH₃CH₃

(**3**); hfac =hexafluoroacetylacetone; NIT-Ph-4-OCHCH₃CH₃ =2-(4-isopropoxyphenyl)-4,4,5,5-tetramethyl-imidazoline-1-oxyl-3-oxide), their crystal structures and magnetic properties were described in detail.

1 Experimental

1.1 Materials and physical measurements

All the starting chemicals were obtained from Aldrich and used without further purification. The radical ligand NIT-Ph-4-OCHCH₃CH₃ was prepared according to literature method^[26]. Elemental analyses (C, H, N) were determined by Perkin-Elmer 240 elemental analyzer. The infrared spectra was recorded from KBr pellets in the range of 4 000~400 cm⁻¹ with a Bruker Tensor 27 IR spectrometer. The magnetic measurements were carried out with MPMSXL-7 SQUID magnetometer. Diamagnetic corrections were made with Pascals constants for all the constituent atoms.

1.2 Synthesis of Complex 1

A solution of Gd(hfac)₃·2H₂O (0.05 mmol) in 25 mL dry heptane was heated to reflux for 2 h. Then the solution was cooled to about 60 °C, a solution of NIT-Ph-4-OCHCH₃CH₃ (0.1 mmol) in 2 mL of CH₂Cl₂ was added. The resulting solution was stirred for about 3 min and then cooled to room temperature. The filtrate was allowed to stand at room temperature for slow evaporation. After three days, some blue crystals were collected. Yield: 31.4 mg (45.5% based on Gd). Elemental analysis calculated for C₄₇H₄₉F₁₈N₄O₁₂Gd(%): C: 41.47; H: 3.63; N: 4.12. Found (%): C: 41.88; H: 3.69; N: 4.22.

1.3 Synthesis of Complex 2

Complex **2** was synthesized with the same procedure for complex **1** using Tb(hfac)₃·2H₂O instead of Gd(hfac)₃·2H₂O. Yield: 32.7 mg (47.9%). Elemental analysis calculated for C₄₇H₄₉F₁₈N₄O₁₂Tb (%): C: 41.42; H: 3.62; N: 4.11. Found (%): C: 40.69; H: 3.57; N: 4.22.

1.4 Synthesis of Complex 3

Complex **3** was synthesized with the same procedure for complex **1** using Dy(hfac)₃·2H₂O instead of Gd(hfac)₃·2H₂O. Yield: 29.3 mg (42.9%). Elemental

analysis calculated for $C_{47}H_{49}F_{18}N_4O_{12}Dy$ (%): C: 41.31; H: 3.61; N: 4.10. Found(%): C: 40.91; H: 3.77; N: 4.17.

1.5 Crystal Structure Determination and Refinement

X-ray single-crystal diffraction data for complexes **1**, **2** and **3** were collected using a Rigaku Saturn CCD diffractometer at 113(2) K with Mo $K\alpha$ radiation ($\lambda = 0.071\ 073$ nm). The structure was solved by direct methods by utilizing the program SHELXS-97^[27] and refined by full-matrix least-squares methods on F^2 with the use of the SHELXL-97 program package^[28]. Anisotropic thermal parameters were assigned to all

non-hydrogen atoms. The hydrogen atoms were set in calculated positions and refined as riding atoms with a common fixed isotropic thermal parameter. Disordered carbon atoms were observed in the hfac ligands for both compounds and disorders were also observed for some fluorine atoms. Pertinent crystallographic data and structure refinement parameters for these complexes were listed in Table 1. Selected bond lengths and bond angles of complexes **1**, **2** and **3** are listed in Table 2.

CCDC: 985443, **1**; 1043098, **2**; 985444, **3**.

Table 1 Crystal data and structure refinement for **1**, **2** and **3**

| Complex | 1 | 2 | 3 |
|-------------------------------|-----------------------------------|-----------------------------------|-----------------------------------|
| Empirical formula | $C_{47}H_{49}F_{18}Gd_1N_4O_{12}$ | $C_{47}H_{49}F_{18}Tb_1N_4O_{12}$ | $C_{47}H_{49}F_{18}Dy_1N_4O_{12}$ |
| Formula weight | 1 361.15 | 1 362.82 | 1 366.40 |
| Crystal system | Triclinic | Monoclinic | Triclinic |
| Space group | $P\bar{1}$ | $P2_1/c$ | $P\bar{1}$ |
| a / nm | 1.219 5(6) | 1.987 2(4) | 1.214 6(10) |
| b / nm | 1.491 9(7) | 1.255 6(3) | 1.489 1(12) |
| c / nm | 1.738 6(7) | 2.282 1(5) | 1.727 6(13) |
| α / (°) | 98.890(5) | 90 | 98.842(6) |
| β / (°) | 103.057(5) | 98.865(5) | 102.753(6) |
| γ / (°) | 111.943(3) | 90 | 111.987(14) |
| V / nm ³ | 2.756(2) | 2.731(4) | 2.728(4) |
| Z | 2 | 4 | 2 |
| D_c / (g·cm ⁻³) | 1.640 | 1.609 | 1.664 |
| μ / mm ⁻¹ | 1.325 | 1.377 | 1.493 |
| R_{int} | 0.062 2 | 0.073 6 | 0.027 2 |
| $F(000)$ | 1 362 | 2 728 | 1 366 |
| Reflections collected | 22 857 | 46 848 | 23 418 |
| Independent reflections | 9 649 | 9 876 | 9 822 |
| GOF on F^2 | 1.017 | 1.032 | 1.021 |
| R_1^a [$I > 2\sigma(I)$] | 0.026 8 | 0.053 2 | 0.037 8 |
| wR_2^b [$I > 2\sigma(I)$] | 0.062 5 | 0.144 5 | 0.091 1 |

$$^a R_1 = \sum (|F_o| - |F_c|) / \sum |F_o|; ^b wR_2 = [\sum w(F_o^2 - F_c^2)^2 / \sum w(F_o^2)]^{1/2}.$$

Table 2 Selected bond distances (nm) and Angles (°) for **1**, **2** and **3**

| 1 | | | | | |
|------------------|------------|------------------|--------------|------------------|------------|
| Gd(1)-O(6) | 0.233 0(8) | Gd(1)-O(7) | 0.233 3(8) | O(2)-N(1) | 0.127 1(3) |
| Gd(1)-O(3) | 0.234 5(7) | Gd(1)-O(9) | 0.235 0(8) | O(6)-N(3) | 0.130 7(3) |
| Gd(1)-O(8) | 0.252 9(8) | Gd(1)-O(12) | 0.239 97(18) | O(3)-N(2) | 0.130 4(2) |
| O(6)-Gd(1)-O(7) | 93.24(7) | O(7)-Gd(1)-O(3) | 105.83(7) | O(11)-Gd(1)-O(9) | 148.80(6) |
| O(6)-Gd(1)-O(11) | 102.93(7) | O(11)-Gd(1)-O(3) | 88.67(7) | O(3)-Gd(1)-O(9) | 73.27(6) |

Continued Table 2

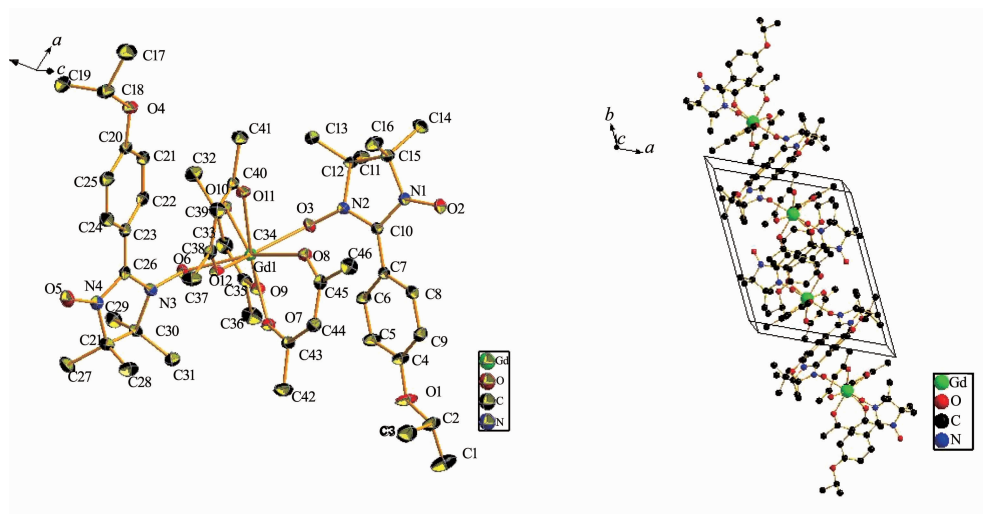
| | | | | | |
|-------------------|------------|-------------------|------------|-------------------|------------|
| O(7)-Gd(1)-O(11) | 136.79(6) | O(6)-Gd(1)-O(9) | 76.52(6) | O(6)-Gd(1)-O(10) | 69.66(7) |
| O(6)-Gd(1)-O(3) | 137.62(6) | O(7)-Gd(1)-O(9) | 73.74(6) | O(7)-Gd(1)-O(10) | 145.23(6) |
| O(11)-Gd(1)-O(10) | 77.69(6) | O(3)-Gd(1)-O(10) | 73.46(6) | | |
| 2 | | | | | |
| Tb(1)-O(4) | 0.234 0(3) | Tb(1)-O(11) | 0.236 0(3) | O(5)-N(4) | 0.127 4(5) |
| Tb(1)-O(2) | 0.234 5(3) | Tb(1)-O(8) | 0.237 4(3) | O(2)-N(2) | 0.131 7(5) |
| Tb(1)-O(7) | 0.234 6(3) | Tb(1)-O(12) | 0.238 1(4) | N(3)-O(4) | 0.131 7(5) |
| O(4)-Tb(1)-O(2) | 137.10(12) | O(2)-Tb(1)-O(11) | 103.35(12) | O(7)-Tb(1)-O(8) | 72.69(13) |
| O(4)-Tb(1)-O(7) | 103.62(13) | O(7)-Tb(1)-O(11) | 137.94(12) | O(11)-Tb(1)-O(8) | 74.01(12) |
| O(2)-Tb(1)-O(7) | 90.96(13) | O(4)-Tb(1)-O(8) | 75.98(12) | O(4)-Tb(1)-O(12) | 149.61(12) |
| O(4)-Tb(1)-O(11) | 92.38(13) | O(2)-Tb(1)-O(8) | 146.60(12) | O(2)-Tb(1)-O(12) | 73.00(12) |
| O(7)-Tb(1)-O(12) | 74.68(13) | O(11)-Tb(1)-O(12) | 72.28(13) | | |
| 3 | | | | | |
| Dy(1)-O(2) | 0.232 1(3) | Dy(1)-O(8) | 0.235 0(3) | O(4)-N(4) | 0.126 9(4) |
| Dy(1)-O(9) | 0.233 5(3) | Dy(1)-O(11) | 0.235 1(3) | O(5)-N(3) | 0.129 7(4) |
| Dy(1)-O(12) | 0.234 6(3) | Dy(1)-O(5) | 0.235 4(3) | O(2)-N(2) | 0.130 4(5) |
| O(2)-Dy(1)-O(9) | 92.77(11) | O(9)-Dy(1)-O(8) | 136.97(11) | O(12)-Dy(1)-O(11) | 74.09(11) |
| O(2)-Dy(1)-O(12) | 69.99(12) | O(12)-Dy(1)-O(8) | 76.91(12) | O(8)-Dy(1)-O(11) | 149.09(11) |
| O(9)-Dy(1)-O(12) | 145.80(11) | O(2)-Dy(1)-O(11) | 76.58(12) | O(2)-Dy(1)-O(5) | 137.83(11) |
| O(2)-Dy(1)-O(8) | 103.30(12) | O(9)-Dy(1)-O(11) | 73.22(11) | O(9)-Dy(1)-O(5) | 105.91(12) |
| O(12)-Dy(1)-O(5) | 73.72(11) | O(8)-Dy(1)-O(5) | 88.47(12) | | |

2 Results and discussion

2.1 Crystal Structure of Complex 1

Single-crystal X-ray diffraction analyses reveal that all these three compounds show similar radical-

Ln(III)-radical structures, which are composed of one Ln(hfac)₃ unit and two NIT-Ph-4-OCHCH₃CH₃ radicals. Compounds **1** and **3** are isostructural and crystallize in the *P* $\bar{1}$ space group, while compound **2** crystallizes in the *P*2₁/*c* space group.



Thermal ellipsoids are drawn at 30% probability; All hydrogen atoms and fluorine atoms are omitted for clarity

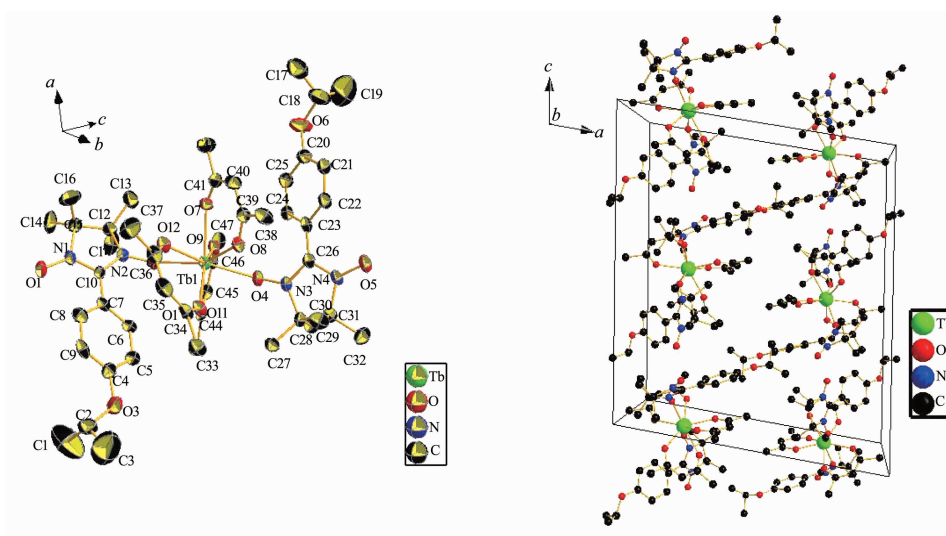
Fig.1 Molecular structure (left) and crystal packing diagram of complex **1** (right)

In complex **1**, the central Gd(III) ions are eight-coordinate with eight oxygen atoms. Two radical ligands bond to one Gd(III) ion via the oxygen atoms of N-O coordination groups. The bond length of Gd(1)-O(6) is 0.234 8 nm while the bond length of Gd(1)-O(3) is 0.237 8 nm. The N(2)-O(3) and N(3)-O(6) bond lengths of nitronyl nitroxide radicals are 0.130 4 nm and 0.130 7 nm, respectively. The uncoordinated N(1)-O(2) and N(4)-O(5) bond lengths are 0.127 1 nm and 0.127 2 nm, respectively, which are comparable to those of reported tri-spin radical-Ln(III)-radical complexes^[29-35]. The other six oxygen atoms are from three hfacs with the Gd-O bond lengths in the range of 0.236 0~0.242 9 nm. The nearest Gd...Gd distance between the adjacent molecules is 1.024 9 nm (Fig.1).

2.2 Crystal structure of complex 2

The crystal structure of complex **2** shows that the

central Tb(III) ions are eight-coordinated with eight oxygen atoms. Two radical ligands bond to one Tb(III) ion via the oxygen atoms of N-O coordination groups. The bond length of Tb(1)-O(4) is 0.234 1 nm while the bond length of Tb(1)-O(2) is 0.234 5 nm. The N(3)-O(4) and N(2)-O(2) bond lengths of nitronyl nitroxide radicals are 0.131 6 nm and 0.131 8 nm respectively. The uncoordinated N(1)-O(1) and N(4)-O(5) bond lengths are 0.128 3 nm and 0.127 3 nm, respectively, which are comparable to those of reported tri-spin radical-Ln(III)-radical complexes^[29-35]. The other six oxygen atoms are from three hfacs with the Tb-O bond lengths in the range of 0.234 6~0.241 7 nm. The nearest Tb...Tb distance between the adjacent molecules is 1.080 8 nm, which is a little bit longer than that for complex **1** (Fig.2).



Thermal ellipsoids are drawn at 30% probability; All hydrogen atoms and fluorine atoms are omitted for clarity

Fig.2 Molecular structure (left) and crystal packing diagram of complex **2** (right)

2.3 Crystal Structure of Complex 3

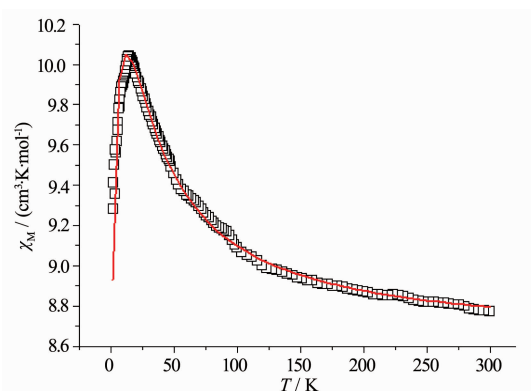
Compound **3** is isostructural to compound **1** and the bond lengths of Dy-O are in the range of 0.232 1~0.239 3 nm, which are a little shorter than the bond lengths of Gd-O.

2.4 Magnetic Properties of Complex 1

Variable-temperature magnetic susceptibilities of complexes **1**, **2**, and **3** were measured from 300 to 2.0 K in an applied field of 1 kOe. The $\chi_M T$ vs T plot for **1** are shown in Fig.3. At 300 K, the $\chi_M T$ value is 8.77

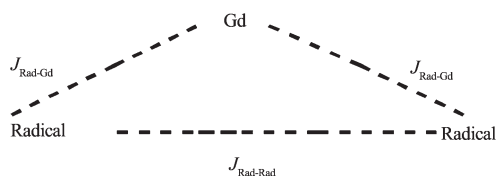
$\text{cm}^3 \cdot \text{K} \cdot \text{mol}^{-1}$, close to the theoretical value of $8.63 \text{ cm}^3 \cdot \text{K} \cdot \text{mol}^{-1}$ (Uncoupled one Gd(III) ion, f^7 electron configuration, $\chi_M T = 7.88 \text{ cm}^3 \cdot \text{K} \cdot \text{mol}^{-1}$ plus two organic radicals ($S = 1/2$, $\chi_M T = 0.375 \text{ cm}^3 \cdot \text{K} \cdot \text{mol}^{-1}$)). Upon cooling, the $\chi_M T$ value of complex **1** increases steadily to a maximum of $10.04 \text{ cm}^3 \cdot \text{K} \cdot \text{mol}^{-1}$ at 15 K, afterward decreases to $9.28 \text{ cm}^3 \cdot \text{K} \cdot \text{mol}^{-1}$ at 2.0 K.

As shown in Scheme 2, there are two kinds of magnetic interactions in this radical-Gd(III)-radical complex at the same time. The first one is Gd(III)-



The solid lines represent the theoretical values based on the corresponding equations

Fig.3 Temperature dependence of $\chi_M T$ for complex 1



Scheme 2 Model of intramolecular interactions

radical interaction and the second one is radical-radical interaction.

The magnetic interactions between Gd(III) and the radicals can be described by isotropic exchange interaction. Thus the experimental data for complex 1 can be analyzed with an expression derived from a spin Hamiltonian. Considering the g value range of the radical and Gd(III) ion, we assume that the radical and Gd(III) ion have the same g value. Thus the variable-temperature magnetic susceptibility data for complex 1 can be analyzed by a theoretical expression (Eq.2) deduced from a spin Hamiltonian (Eq.1)^[30-35].

The best fitting leads to $g=2.00$, $J_{\text{Rad-Gd}}=2.57 \text{ cm}^{-1}$, $J_{\text{Rad-Rad}}=-9.98 \text{ cm}^{-1}$ for complex 1. The positive value of $J_{\text{Rad-Gd}}$ indicates that there is a weak ferromagnetic interaction between the Gd(III) and the radicals in the molecule. The negative $J_{\text{Rad-Rad}}$ indicates the antiferromagnetic interaction between the two intramolecular radicals. The obtained J value is comparable with the previously reported Gd^{III}-radicals compounds^[30-35].

$$H = -2J_{\text{Rad-Gd}}(\hat{S}_{\text{Rad1}} \cdot \hat{S}_{\text{Gd}} + \hat{S}_{\text{Rad2}} \cdot \hat{S}_{\text{Gd}}) - 2J_{\text{Rad-Rad}}\hat{S}_{\text{Rad2}} \cdot \hat{S}_{\text{Rad1}} \quad (1)$$

$$\chi_M = \frac{Ng^2\beta^2}{kT} \frac{A}{B}$$

$$A = 165 + 84\exp\left(-\frac{9J_{\text{Rad-Gd}}}{kT}\right) + 84\exp\left(-\frac{7J_{\text{Rad-Gd}} + 2J_{\text{Rad-Rad}}}{kT}\right) + 35\exp\left(-\frac{16J_{\text{Rad-Gd}}}{kT}\right)$$

$$B = 5 + 4\exp\left(-\frac{9J_{\text{Rad-Gd}}}{kT}\right) + 4\exp\left(-\frac{7J_{\text{Rad-Gd}} + 2J_{\text{Rad-Rad}}}{kT}\right) + 3\exp\left(-\frac{16J_{\text{Rad-Gd}}}{kT}\right) \quad (2)$$

2.5 Magnetic properties of complex 2

While for complex 2 (Fig.4), at 300 K, the $\chi_M T$ value is $13.08 \text{ cm}^3 \cdot \text{K} \cdot \text{mol}^{-1}$, close to the theoretical value $12.57 \text{ cm}^3 \cdot \text{K} \cdot \text{mol}^{-1}$ in uncoupled system of one Tb(III) ion (f^9 electron configuration, $\chi_M T=11.82 \text{ cm}^3 \cdot \text{K} \cdot \text{mol}^{-1}$) plus two organic radical ($S=1/2$, $\chi_M T=0.375 \text{ cm}^3 \cdot \text{K} \cdot \text{mol}^{-1}$). Upon cooling, the $\chi_M T$ value of complex 2 increases steadily to a maximum of $28.62 \text{ cm}^3 \cdot \text{K} \cdot \text{mol}^{-1}$ at 3.0 K, afterward the value decreases to $28.54 \text{ cm}^3 \cdot \text{K} \cdot \text{mol}^{-1}$ at 2.0 K. The increase of $\chi_M T$ suggests the presence of ferromagnetic interaction between the Tb(III) and the organic radical. The decrease of $\chi_M T$ at low temperature indicates the antiferromagnetic interaction between the two intramolecular radicals. The magnetic properties of complex 2 are similar to those of previously reported^[29-35].

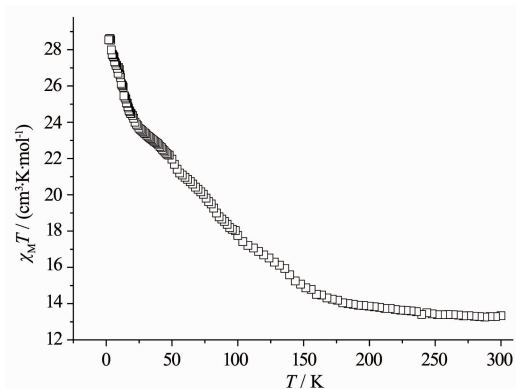


Fig.4 Temperature dependence of $\chi_M T$ for complex 2

Alternating current (ac) susceptibility measurements for complex 2 were carried out in low temperature regime under a zero dc field to investigate the dynamics of the magnetization. As shown in Fig.5, there are no obvious frequency dependent out-of-phase signals. We do not think that complex 2 express SMM behavior at low temperature. This may due to

the small energy barrier which could not prevent the inversion of spin.

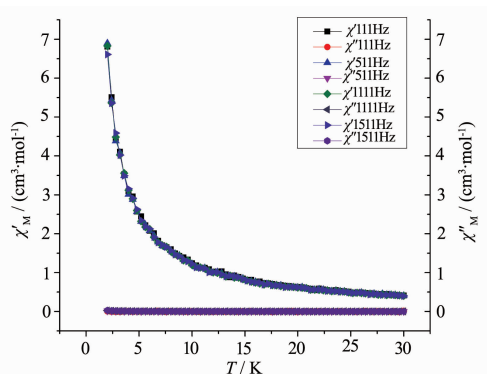


Fig.5 Temperature dependence of the in-phase and out-of-phase components of ac susceptibility for **2** in zero dc field with an oscillation of 3.5 Oe

2.6 Magnetic properties of complex 3

Complex **3** shows similar magnetic properties with complex **1** (Fig.6). At 300 K, the $\chi_M T$ value is $15.01 \text{ cm}^3 \cdot \text{K} \cdot \text{mol}^{-1}$, close to the theoretical value of $14.92 \text{ cm}^3 \cdot \text{K} \cdot \text{mol}^{-1}$. Upon cooling, the $\chi_M T$ value of complex **3** increases steadily to a maximum of $19.79 \text{ cm}^3 \cdot \text{K} \cdot \text{mol}^{-1}$ at 15.4 K, afterward decreases to $16.97 \text{ cm}^3 \cdot \text{K} \cdot \text{mol}^{-1}$ at 2.0 K. The plot also suggests the presence of ferromagnetic interaction between the Dy(III) and the coordinated N-O groups of the organic radicals and the antiferromagnetic interaction between the two intramolecular radicals.

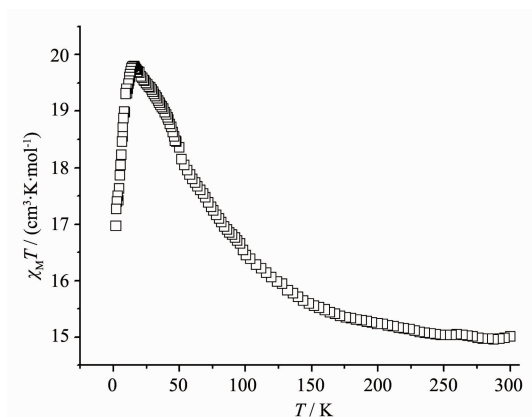


Fig.6 Temperature dependence of $\chi_M T$ for complexes **3**

Alternating current (ac) susceptibility measurements for complex **3** were also carried out in low temperature regime under a zero dc field. The result (Fig.7) shows that there are no obvious frequency dependent out-of-phase signals. Like complex **2**,

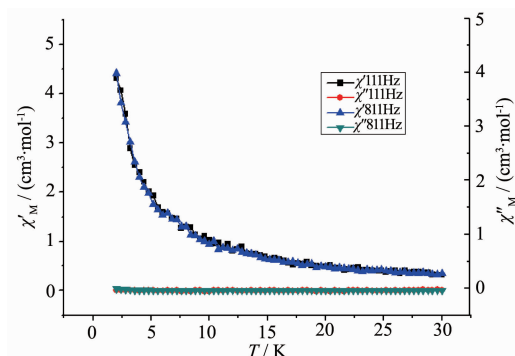


Fig.7 Temperature dependence of the in-phase and out-of-phase components of ac susceptibility for **3** in zero dc field with an oscillation of 3.5 Oe

complex **3** does not express SMMs behavior at low temperature.

3 Conclusions

A novel nitronyl nitroxide radical and its three corresponding mononuclear tri-spin compounds $\text{Ln}(\text{hfac})_3(\text{NIT-Ph-4-OCHCH}_3\text{CH}_3)_2$ ($\text{Ln}=\text{Gd}$ (**1**), Tb (**2**), Dy (**3**)) have been synthesized and characterized. The magnetic studies reveal that ferromagnetic interactions (between the intramolecular Ln and radical) and antiferromagnetic interactions (between the intramolecular radicals) are coexist in these complexes. Complexes **2** and **3** do not have SMMs behavior at low temperature, this may due to the small energy barrier which could not prevent the inversion of spin.

References:

- [1] Kahn O. *Molecular Magnetism*. New York: Wiley-VCH, **1993**.
- [2] Moller S, Perlov C, Jackson W, et al. *Nature*, **2003**,**426**:166-169
- [3] Kahn M L, Sutter J P, Golhen S, et al. *J. Am. Chem. Soc.*, **2000**,**122**:3413-3421
- [4] Zhang P, Guo Y N, Tang J K. *Coord. Chem. Rev.*, **2013**,**257**: 1728-1737
- [5] Ruiz-Molina D, Mas-Torrent M, Gómez J, et al. *Adv. Mater.*, **2003**,**15**:42-49
- [6] Clemente-León M, Soyer H, Coronado E, et al. *Angew. Chem. Int. Ed.*, **1998**,**37**:2842-2845
- [7] Cornia A, Fabretti A C, Pacchioni M, L, et al. *Angew. Chem. Int. Ed.*, **2003**,**42**:1645-1651
- [8] Gatteschi D, Caneschi A, Pardi L, et al. *Science*, **1994**,**265**:

- 1054-1058
- [9] Bar A K, Pichon C, Gogoi N, et al. *Chem. Commun.*, **2015**, **51**:3616-3619
- [10] Liu R N, Li L C, Wang X L, et al. *Chem. Commun.*, **2010**, **46**:2566-2570
- [11] Bogani L, Wernsdorfer W. *Nat. Mater.*, **2008**, **7**:179-183
- [12] Caneschi A, Gatteschi D, Lalioti N, et al. *Angew. Chem. Int. Ed.*, **2001**, **40**:1760-1793
- [13] Bogani L, Sangregorio C, Sessoli R, et al. *Angew. Chem. Int. Ed.*, **2005**, **44**:5817-5821
- [14] Bernot K, Luzon J, Bogani L, et al. *J. Am. Chem. Soc.*, **2009**, **131**:5573-5579
- [15] Liu J L, Wu J Y, Chen Y C, et al. *Angew. Chem. Int. Ed.*, **2014**, **53**:12966-12970
- [16] Chatelain L, Walsh J P S, Pecaut J, et al. *Angew. Chem. Int. Ed.*, **2014**, **53**:13434-13439
- [17] Zhang P, Zhang L, Wang C. *J. Am. Chem. Soc.*, **2014**, **136**:4484-4489
- [18] Poneti G, Bernot K, Bogani L, et al. *Chem. Commun.*, **2007**, 1807-1809
- [19] Rinehart J D, Fang M, Evans W J, et al. *J. Am. Chem. Soc.*, **2011**, **133**:14236-14239
- [20] Rinehart J D, Fang M, Evans W J, et al. *Nat. Chem.*, **2011**, **3**:538-542
- [21] Chernick E T, Casillas R, Zirzlmeier J, et al. *J. Am. Chem. Soc.*, **2015**, **137**:857-863
- [22] Mailman A, Winter S M, Wong J W L, et al. *J. Am. Chem. Soc.*, **2015**, **137**:1044-1049
- [23] Wang X F, Hu P, Li Y G, et al. *Chem. Asian J.*, **2015**, **10**:325-330
- [24] Zhu M, Hu P, Li Y, et al. *Chem. Eur. J.*, **2014**, **20**:13356-13364
- [25] Wang Z X, Zhang X, Zhang Y Z, et al. *Angew. Chem. Int. Ed.*, **2014**, **53**:11567-11570
- [26] Ullman E F, Osiecki J H, Boocock D G B, et al. *J. Am. Chem. Soc.*, **1972**, **94**:7049-7059
- [27] Sheldrick G M. *SHELXS-97: Program for the Solution of Crystal Structures*, University of Göttingen, Germany, **1997**.
- [28] Sheldrick G M. *SHELXL-97: Program for the Refinement of Crystal Structures*, University of Göttingen, Germany, **1997**.
- [29] Hu P, Zhang C, Gao Y, et al. *Inorg. Chim. Acta*, **2013**, **398**:136-140
- [30] Zhou N, Ma Y, Wang C, et al. *Dalton Trans.*, **2009**:8489-8492
- [31] Wang C, Wang Y L, Qin Z X, et al. *Inorg. Chem. Commun.*, **2012**, **20**:112-117
- [32] Zhang C X, Chen H W, Wang W M, et al. *Inorg. Chem. Commun.*, **2012**, **24**:177-181
- [33] Du F X, Hu P, Gao Y Y, et al. *Inorg. Chem. Commun.*, **2014**, **48**:166-170
- [34] Zhang C X, Qiao X M, Kong Y K, et al. *J. Mol. Struct.*, **2015**, **108**:1348-1354
- [35] Li L L, Liu S, Zhang Y, et al. *Dalton Trans.*, **2015**, **44**:6118-6125